

## Dual-band infrared single-layer metallodielectric photonic crystals

Robert P. Drupp, Jeremy A. Bossard, Yong-Hong Ye,  
Douglas H. Werner, and Theresa S. Mayer<sup>a)</sup>

*Department of Electrical Engineering, Center for Nanoscale Science, The Pennsylvania State University,  
University Park, Pennsylvania 16802*

(Received 17 March 2004; accepted 2 July 2004)

Metallodielectric photonic crystals (MDPCs) consisting of periodic arrays of self-similar two-stage fractal patch metallic elements patterned on thin dielectric substrates are shown to exhibit excellent mid- and far-infrared dual-band response in a single layer structure. This was achieved by optimizing the element size and interelement spacing of cross-dipole and square-patch fractal elements using full-wave periodic method of moments modeling techniques that calculate electromagnetic scattering from the MDPC surface and are able to account for material loss and loading effects. All structures fabricated based on these designs had two measured stopbands with greater than 10 dB attenuation positioned at wavelengths determined by element geometry and size as well as interelement spacing. This simple single layer fractal MDPC geometry will facilitate further scaling into the near-IR wavelength regime. © 2004 American Institute of Physics.

[DOI: 10.1063/1.1786663]

Metallodielectric photonic crystals (MDPCs) are being investigated as IR band-reject and band-pass filters for use in low-cost, high-performance devices including beam-splitters, filters, and polarizers.<sup>1</sup> Traditionally, such MDPCs were fabricated by stacking three or more layers of micron-scale metallic patch elements with intermediate dielectric spacers to achieve structures having a single resonant stopband with requisite band rejection properties ( $>10$  dB).<sup>2-4</sup> More recently, MDPCs consisting of a dielectric substrate supporting a single planar periodic array of metallic patch elements, such as coupled<sup>5</sup> or uncoupled<sup>6</sup> dipoles, cross-dipoles,<sup>7</sup> and rings,<sup>8</sup> have also been demonstrated. Currently, there is growing interest in extending the filtering capabilities of both multilayer<sup>9</sup> and single-layer MDPCs to include multiband responses.<sup>10</sup> In this letter, we report on the design and experimental verification of MDPCs that utilize simple, self-similar fractal metallic patch elements patterned on a thin dielectric substrate to achieve excellent mid- and far-IR dual-band rejection in a single-layer structure.

Electromagnetically coupled arrays of fractal elements have been used previously in filtering applications at micro- and millimeter wave frequencies, where the structures are often referred to as frequency selective surfaces (FSSs). Similar concepts can be applied in the IR due to the scalable nature of electromagnetic theory used to predict the spectral response of these filters. Although many different fractal geometries can be conceived, we have chosen to study MDPCs comprised of arrays of simple two-stage cross-dipole<sup>11</sup> and square-patch fractal metallic elements<sup>12</sup> shown in Fig. 1 to demonstrate the utility of this approach at IR wavelengths. The dual-band response of these MDPCs is associated with two resonances resulting from the self-similar primary and secondary structure of the fractal elements. In addition, the radial symmetry of these elements gives rise to a response that is relatively insensitive to wave polarization and angle of incidence. Here we show through modeling and experiment that the two stopband rejection wavelengths and their rela-

tive attenuation are strongly dependent on element geometry and interelement spacing.

Theoretical design and modeling of the single- and dual-band MDPCs was performed using a full-wave periodic method of moments (PMM) technique that calculates electromagnetic scattering from the MDPC surface to determine the transmitted power as a function of wavelength and polarization of the incident radiation.<sup>13</sup> Briefly, the PMM technique is based on developing an integral equation for a single unit cell (i.e., cross-dipole or square-patch element) that is modified for a periodic array of cells by applying Floquet's theorem.<sup>14</sup> This modified integral equation is discretized into a system of linear equations by applying a subdomain method of moments approach with rooftop basis functions to

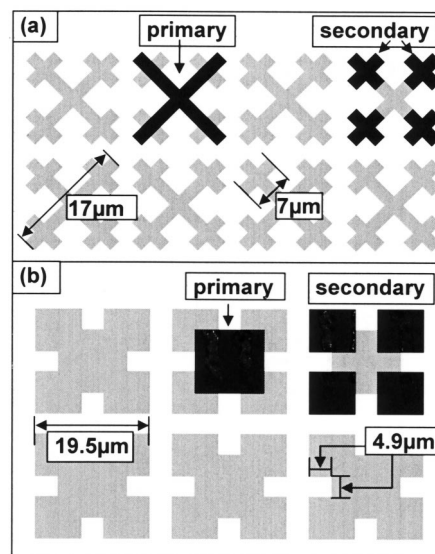


FIG. 1. Drawing of periodic array of fractal metallic patch elements with primary and secondary structures highlighted on successive elements: (a) fractal cross-dipole elements with interelement spacing of  $1.2 \mu\text{m}$ , (b) fractal square-patch elements with interelement spacing of  $6.5 \mu\text{m}$ . In this letter, the fractal element size and interelement spacing are varied to investigate their role on stopband attenuation and position.

<sup>a)</sup>Electronic mail: tsm2@psu.edu

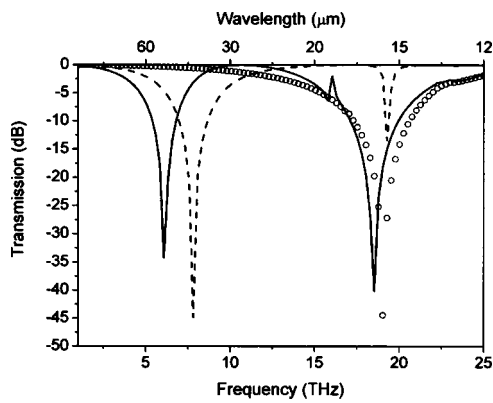


FIG. 2. Ideal PMM simulations for fractal cross-dipole elements with optimized spacing (solid curve) show two strong stop bands. Ideal simulations for primary and secondary single cross-dipoles (dashed curve and circles) each show a single strong stop band indicating that each stage of the fractal structure causes one stop band.

determine the unknown current distributions in the elements and hence the scattering from the MDPC surface. The effects of metallic and dielectric loss can be readily incorporated into this PMM formulation and will be included here to provide a comparison with experimental data collected on several MDPCs.

The PMM method was used to model the spectral response of an IR-sensitive two-stage fractal cross-dipole MDPC and optimize the interelement spacing to simultaneously maximize attenuation in both stopbands. Design optimization was conducted assuming ideal lossless metal elements and a thin, lossless substrate (i.e., less than  $1/20$  of the shortest resonant wavelength). We selected unit cell elements with primary and secondary cross-dipole arm lengths of 17 and 7  $\mu\text{m}$  and linewidth of 1.5  $\mu\text{m}$  to facilitate rapid fabrication of the MDPC using optical contact lithography. The resulting transmission spectrum for a dual-band MDPC with an optimized interelement spacing is shown as a solid line in Fig. 2. An interelement spacing of 1.2  $\mu\text{m}$  provides nearly equal attenuation of 34 and 40 dB in the primary and secondary stopbands centered at 49 and 16  $\mu\text{m}$ , respectively. Although not shown, we found that larger and smaller spacing increases the attenuation of one band at the expense of the other band because the amount of electromagnetic coupling between elements of a particular spacing is extremely sensitive to the wavelength of the incident radiation. For example, a larger 2.2  $\mu\text{m}$  interelement spacing increased the attenuation in the secondary band to 44 dB while reducing the primary band to 25 dB. Decreasing the spacing to 0.8  $\mu\text{m}$  had the opposite effect, where the attenuation in the primary band increased to 46 dB and secondary band decreased to 31 dB. In both cases, the primary and secondary stopband positions remained unchanged.

PMM-simulated transmission spectra of nonfractal cross-dipole MDPCs with dimensions and spacing identical to the primary and secondary crosses of the optimized fractal structure are also included as a dashed line and open circles in Fig. 2 for comparison. The array of single 17- $\mu\text{m}$ -long elements has a single stop band with an attenuation of 45 dB centered at 40  $\mu\text{m}$ , which occurs at a significantly shorter wavelength than the corresponding primary band of the fractal cross-dipole MDPC. The redshift in the primary band of the fractal structure is due to loading of the primary crosses by the secondary crosses, which electrically lengthen the pri-

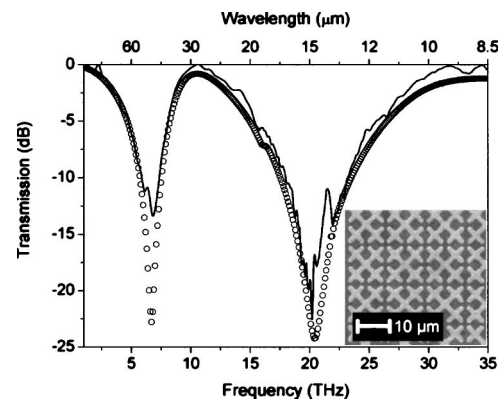


FIG. 3. Comparison of measured (solid curve) and simulated (circles) transmission spectra for fractal cross-dipole elements with optimized interelement spacing of 1.2  $\mu\text{m}$ . Measured primary and secondary stop bands have attenuation of 13 and 23 dB centered at 44 and 15  $\mu\text{m}$ , respectively. For reference, MDPCs of the same geometry fabricated using a single 75-nm-thick layer of silver as the metal patch elements exhibited a response that is nearly identical to those fabricated using aluminum (shown here). The PMM model includes the effects of metallic and dielectric loss.

mary crosses making them resonant at a longer wavelength. This same effect is observed to a lesser extent for the array of single 7- $\mu\text{m}$ -long cross-dipole elements where a single stop band with an attenuation of 44 dB is centered at 16  $\mu\text{m}$ . This analysis clearly demonstrates that the self-similarity of the fractal structure gives rise to a dual-band response in a single layer of metallic patch elements.

The optimized fractal cross-dipole MDPC was fabricated by defining a  $1 \times 1 \text{ cm}^2$  array of 75-nm-thick aluminum elements on top of a 0.5- $\mu\text{m}$ -thick IR-transparent polyimide film. Aluminum was selected for these studies because it adheres well to the polyimide film and has low loss in the far-IR wavelength regime.<sup>15</sup> The polyimide is deposited by spin coating onto a sacrificial substrate that is removed prior to spectral characterization of the MDPC in the mid- and far-IR. Transmission spectra are collected with the sample at normal incidence to the IR beam using a Bruker Optics Equinox 55 Fourier Transform Infrared spectrometer and normalized to the background of the substrate. The measured and modeled transmission spectra for the MDPC are shown as the solid curve and open circles in Fig. 3. The measured spectrum contains strong primary and secondary stopbands with attenuation of approximately 13 and 23 dB centered at 44 and 15  $\mu\text{m}$ , respectively. This is in excellent agreement with the modeled response shown in Fig. 3, which includes the effect of metallic and dielectric loss. This simulation incorporated measured values of frequency-dependent aluminum loss for the metallic patch elements,<sup>15</sup> and a frequency-independent complex dielectric constant  $\epsilon_r = 3.0 - 0.3j$  for the dielectric loss associated with the substrate.<sup>16</sup> In comparison to the ideal case of Fig. 2, the metallic and dielectric loss result in a reduction in the attenuation in each stopband, and cause small shifts in band positions.

A fractal square patch geometry was also studied to demonstrate that dual-band response can be achieved with different fractal structures. A MDPC was designed using PMM modeling to have stopbands at the same wavelengths as the cross-dipole structure in Fig. 3. The resulting two-stage fractal array has primary and secondary square patches that are 9.8 and 7.3  $\mu\text{m}$  wide, with an interelement spacing of 6.5  $\mu\text{m}$ . The measured and modeled transmission spectra

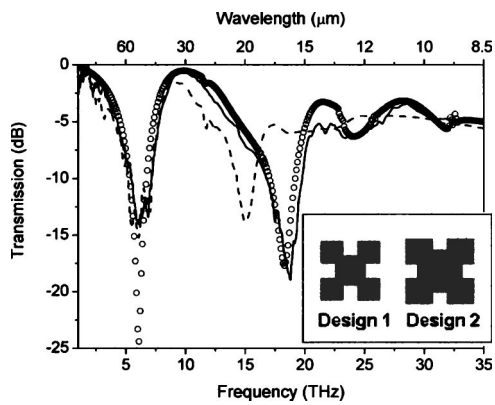


FIG. 4. Measured transmission spectrum of design 1 of the fractal square patch (solid curve) agrees well with the model prediction (circles curve) and contains two strong stop bands at the same positions as those in the fractal cross-dipole case. Design 2 of the fractal square patch (dashed curve) demonstrates that the position of one stop band can be changed relative to the other by adjusting the element geometry and interelement spacing.

shown as solid curve and open circles in Fig. 4 demonstrate that the targeted stopband wavelengths were obtained with strong primary and secondary band attenuation of approximately 14 and 19 dB at 50 and 16  $\mu\text{m}$ . Once again, there is excellent agreement between the measured and modeled spectral response when the same values of metallic and dielectric loss used for the cross-dipole structure are included in the simulation.

Modeling of fractal FSSs in the micro- and millimeter wave regime has shown that the position of all stopbands can be shifted by the same amount by changing element size while maintaining similarity. It is also possible to scale the relative dimensions of the primary and secondary fractal structures to adjust one band position with respect to the other band. We redesigned the two-stage square patch MDPC such that the primary band remained at a wavelength of 50  $\mu\text{m}$  and the secondary band shifted to a longer wavelength of 20  $\mu\text{m}$ . Contrary to what might be expected without considering element loading effects, it was determined that both the primary and secondary square patch elements must increase in size to 15 and 9  $\mu\text{m}$ , respectively, with an interelement spacing of 9.2  $\mu\text{m}$ . The measured transmission spectrum shown as the dashed curve in Fig. 4 demonstrates that the primary stopband wavelength is unchanged, and the secondary wavelength is shifted to 20  $\mu\text{m}$  with 14 dB attenuation. This design process underscores the importance of the PMM modeling to fully account for the complex loading effects that significantly impact the spectral properties of the MDPC.

In conclusion, dual-band IR MDPCs that are comprised of a single layer of self-similar cross-dipole or square-patch

fractal metallic elements were investigated theoretically and experimentally. Modeling and design optimization were conducted using a full-wave PMM technique that accounts for element and dielectric loss as well as element loading effects. It was determined that the band rejection wavelengths and their relative attenuation are strongly dependent on element geometry and interelement spacing. MDPCs fabricated using aluminum elements and thin polyimide substrates had measured transmission spectra that were in excellent agreement with the modeled response. In all cases the attenuation in the stopbands exceeded the targeted value of 10 dB required for most high performance applications. These results show that simple fractal geometries can be used to achieve excellent IR multiband behavior using a single layer of metallic patch elements, which will facilitate further scaling into the mid- and near-IR wavelength regime using imprint lithographic techniques.<sup>17</sup>

This research was supported by the NSF MRSEC, Center for Nanoscale Science, Grant No. DMR-0213623. R.D. acknowledges support from a Materials Research Institute Graduate Fellowship. The authors also acknowledge the Penn State Materials Characterization Laboratory for SEM facilities.

- <sup>1</sup>I. Puscasu, G. Boreman, R. C. Tiberio, D. Spencer, and R. R. Krchnavek, *J. Vac. Sci. Technol. B* **18**, 3578 (2000).
- <sup>2</sup>E. R. Brown and O. B. McMahon, *Appl. Phys. Lett.* **60**, 2138 (1995).
- <sup>3</sup>J. S. McCalmont, M. M. Sigalas, G. Tuttle, K.-M. Ho, and C. M. Soukoulis, *Appl. Phys. Lett.* **68**, 2759 (1996).
- <sup>4</sup>E. Z. Ozbay, B. Temelkuran, M. Sigalas, G. Tuttle, C. M. Soukoulis, and K. M. Ho, *Appl. Phys. Lett.* **69**, 3797 (1996).
- <sup>5</sup>I. Puscasu, W. L. Schaich, and G. D. Boreman, *Appl. Opt.* **40**, 118 (2001).
- <sup>6</sup>I. Puscasu, D. Spencer, and G. D. Boreman, *Appl. Opt.* **39**, 1570 (2000).
- <sup>7</sup>H. A. Smith, M. Rebbert, and O. Sternberg, *Appl. Phys. Lett.* **82**, 3605 (2003).
- <sup>8</sup>S. J. Spector, D. K. Astolfi, S. P. Doran, T. M. Lyszczarz, and J. E. Reynolds, *J. Vac. Sci. Technol. B* **19**, 2757 (2001).
- <sup>9</sup>J. A. Oswald, B.-I. Wu, K. A. McIntosh, L. J. Mahoney, and S. Verghese, *Appl. Phys. Lett.* **77**, 2098 (2000).
- <sup>10</sup>W. Wen, Z. Yang, G. Xu, Y. Chen, L. Zhou, W. Ge, C. T. Chan, and P. Sheng, *Appl. Phys. Lett.* **83**, 2106 (2003).
- <sup>11</sup>D. H. Werner and S. Ganguly, *IEEE Antennas Propag. Mag.* **45**, 38 (2003).
- <sup>12</sup>J. P. Gianvittorio, Y. Rahmat-Samii, and J. Romeu, *Proceedings of the IEEE International Symposium on Antennas and Prop.*, Boston, MA, 2001, Vol. 3, pp. 640–643.
- <sup>13</sup>T. K. Wu, *Frequency Selective Surface and Grid Array* (Wiley, New York, 1995).
- <sup>14</sup>R. Mittra, C. H. Chan, and T. Cwik, *Proc. IEEE* **76**, 1593 (1988).
- <sup>15</sup>A. Rakic, A. Djuricic, J. Elazar, and M. Majewski, *Appl. Opt.* **37**, 5271 (1998).
- <sup>16</sup>Z. M. Zhang, G. Lefever-Burton, and F. R. Powell, *Int. J. Thermophys.* **19**, 905 (1998).
- <sup>17</sup>T. C. Bailey, S. C. Johnson, S. V. Sreenivasan, J. G. Ekerdt, C. G. Willson, and D. J. Resnick, *J. Photopolym. Sci. Technol.* **15**, 481 (2002).